

Article

Development of an ANN-Based Lumped Plasticity Model of RC Columns Using Historical Pseudo-Static Cyclic Test Data

Zhenliang Liu ^{1,2} and Suchao Li ^{1,2,3,*} 

- ¹ Key Laboratory of Structural Dynamic Behavior and Control of Ministry of Education, School of Civil Engineering, Harbin Institute of Technology, Harbin 150090, China; 15B933009@hit.edu.cn
- ² Key Lab of Smart Prevention and Mitigation of Civil Engineering Disasters of Ministry of Industry and Information Technology, Harbin Institute of Technology, Harbin 150090, China
- ³ Department of Civil Engineering, Harbin Institute of Technology at Weihai, Weihai 264209, China
- * Correspondence: lisuchao@hit.edu.cn; Tel.: +86-1363-360-1698

Received: 19 September 2019; Accepted: 5 October 2019; Published: 11 October 2019



Featured Application: Predicting the critical properties of RC columns using the developed ANN model, providing parameters for their numerical simulation based upon a lumped plasticity model.

Abstract: This study explores the possibility of using an ANN-based model for the rapid numerical simulation and seismic performance prediction of reinforced concrete (RC) columns. The artificial neural network (ANN) method is implemented to model the relationship between the input features of RC columns and the critical parameters of the commonly used lumped plasticity (LP) model: The strength and the yielding, capping and ultimate deformation capacity. Cyclic test data of 1163 column specimens obtained from the PEER and NEESHUB database and other sources are collected and divided into the training set, test set and validation set for the ANN model. The effectiveness of the proposed ANN model is validated by comparing it with existing explicit formulas and experimental results. Results indicated that the developed model can effectively predict the strength and deformation capacities of RC columns. Furthermore, the response of two RC frame structures under static force and strong ground motion were simulated by the ANN-based, bi-linear and tri-linear LP model method. The good agreement between the proposed model and test results validated that the ANN-based method can provide sufficiently accurate model parameters for modeling the seismic response of RC columns using the LP model.

Keywords: strength; yielding capping and ultimate deformation; RC column; cyclic test database; artificial neural network; bi-linear and tri-linear lumped plasticity model

1. Introduction

Reinforced concrete (RC) columns are fundamental structural components that are widely used in civil infrastructures such as buildings and bridges. In seismic-prone regions, the seismic performance of such structural components significantly affects structural safety in seismic events. However, due to the nonlinearity of structural materials and the uncertainty of earthquake excitations, there are still some difficulties exists for researchers and engineers in some fields, e.g., the rapid seismic evaluation of a regional transport network, including a number of bridges [1]. Therefore, it is still necessary to develop a rapid and reliable model for the main components of structures, e.g., RC columns and piers.

Researchers and engineers in seismic engineering have conducted many laboratory experiments, including pseudo-static and shaking table tests, to investigate the mechanical properties of RC columns. Based on them, several explicit formulas have also been established, founded upon a

theoretical analysis and regression analysis of experimental data [2,3] for structural design in seismic engineering. Priestley et al. [4] examined existing design equations related to shear strength, and observed significant differences in the predicted results. Sezen and Moehle [5] and Elwood and Moehle [6] also found significant inaccuracies in the predicted deformation capacity of RC columns obtained from existing methods. The reason for the differences is that RC material exhibits strong uncertainties and nonlinearity. Moreover, under the combination of constant vertical and lateral dynamic loads, the seismic performance of RC columns is affected by many other properties of structural components, such as the shear span ratio [7], longitudinal and transverse reinforcement ratio [8,9] and the axial compression ratio [10].

Besides, finite element analysis (FEA) is an alternative and useful tool that can be used to analyze the nonlinear mechanical properties of the RC structure [11,12]. For RC columns, the lumped plasticity (LP) hinge method and distributed plasticity (DP) hinge method are typical methods to model the nonlinear characteristics of the structures [13,14]. However, the LP method is relatively coarse, while the DP method is often time-consuming, and the results significantly depend upon the setup of the model parameters and boundary conditions [15]. This may lead to large estimation errors during the seismic performance prediction of RC structures. Lu et al. [16] organized an open competition to predict the hysteretic response of a 3-storey frame, which was initially tested in the laboratory. Although detailed information of the structural configuration and material properties was provided to the competitors, most of the FEA results of 30 research groups were far from the test results, no matter what types of FEA model they used. This may result from the complicated damage mechanism of the material and the unclear boundaries and connections in the real RC structures. To overcome these drawbacks, Ibarra et al. [17] developed a relatively simple LP model including the effective stiffness, pre and post-peak inelastic deformations, etc. It has been demonstrated that this model can simulate the seismic performance of RC structures with proper model parameters [18,19]. In practice, the accurate analysis is not only dependent upon the tools used, but also the experience of the analysts (mainly from the disaster lessons or the laboratory test results). The experience, which is generally related to the model parameter determination, may vary greatly among different groups. Therefore, essential model parameters considering the historical experience are needed for the accurate simulation of RC columns. In this study, a model-free and data-driven method is deduced for the determination of the key parameters of the commonly-used LP model. It is expected that more test results can overcome subjective errors and model uncertainties, improving the LP model.

An artificial neural network (ANN) is a typical machine learning (ML) method, which was inspired by the architecture and operation of biological nervous systems. Recently, they have been adopted by researchers in civil engineering, such as investigating energy performances [20]. Kawashima and Oreta [21] validated the application of ANN models in simulating the compressive stress–strain relationship, especially with limited data. In addition, other non-parametric models, the conditional average estimator (CAE) method [22] and support vector machine (SVM) [23], were also employed by researchers to analyze the mechanical properties or seismic performance of structures. González and Zapico [24] presented a seismic damage identification method for a steel moment–frame structure based on modal variables, and Reza et al. [25] conducted a detailed parametric study on the limiting states of bridge columns using factorial analysis. Compared with current existing formulas based on the regression algorithm or experiences, the ANN-based model, originating from an advanced humanlike information processing style, is data-driven. It only relies on a large quantity of training data with sufficient features of the samples rather than a limited database and certain assumptions, and thus it can help to reduce some subjective and experimental errors and be more reliable. Nevertheless, their application in engineering is still limited, and so this study conducted a pioneer study on developing an ANN-based LP model for the seismic assessment of RC columns. It investigates the possibility of predicting the important model properties of RC columns using an ANN model and a large quantity of historical test results.

Data is fundamental to the application of machine learning technology. The accumulation of numerous cyclic experiments in RC columns can provide an alternative approach to predict their seismic performance using a model-free method. In this study, the data collection criteria and experimental data for training, testing and validating the ANN model of the RC columns are briefly introduced in the first Section. Then, the ANN architecture, including the input, output and hidden layer, is described specifically. Subsequently, the ANN model is validated using a test set and some existing explicit formulas developed by other researchers. Finally, a comparison investigation is conducted on two RC frame structures between the ANN-based LP method with a quasi-static and a shaking table test. This well-trained, ANN-based LP method in this paper is also implemented in an efficient Matlab graphical user interface (GUI), which could be directly used for structural performance evaluation or response prediction by other researchers or engineers during their investigation.

2. Data Collection

Researchers worldwide have conducted numerous pseudo-static cyclic tests on RC columns to investigate the hysteretic behavior and seismic performance of such structural components in buildings and bridges. To provide data for training the ANN model, the cyclic test results of RC columns were collected from the NEEShub database [26], PEER database [27] and other published studies based upon the following criteria:

1. The shape of the cross section of the RC columns should be rectangular; others like circular columns are not included in this study.
2. The RC columns only sustained constant axial loading and unidirectional cyclic lateral force. Cyclic tests of the RC column under biaxial lateral or variable axial loads are excluded.
3. A complete loading process was applied to the specimens until failure; the load carrying capacity of the specimen decreased by more than 20% compared to the peak strength.
4. Details of the specimens are available, such as the geometrical size and reinforcement, as well as experimental results of the hysteretic curves.
5. Normal concrete was used in the manufacture of the specimens, without additives such as steel fiber.

A total of 1163 cyclic test results of RC columns were collected to build a database for training, testing and validating the ANN model. Details of the selected specimens, including the data source and geometrical size, are listed in the Appendix A. It can be observed that the main features of the selected columns have a relatively wide distribution.

The numerical simulation of RC columns may depend upon many factors, such as the material properties, geometrical configuration, reinforcement layout and loading protocol. Figure 1 shows a schematic diagram of a typical cantilever column, illustrating some of these factors, as well as its LP model. The section width (B) and depth (D) is defined as the section size which is perpendicular and parallel to the lateral force, respectively. It should be noted that a cantilever and fixed-end columns are two typical structural components used for civil structures. For simplicity, this study mainly focused on cantilever columns, which are widely used in bridge piers; the geometrical size and test results of the fixed-end columns were modified by assuming that the inflection point of the columns occurs at the half height of the column. As illustrated, the optimal feature subset is selected by the genetic algorithm (GA) method, then used to train the ANN model. It can help determine the parameters of the LP model for RC columns.

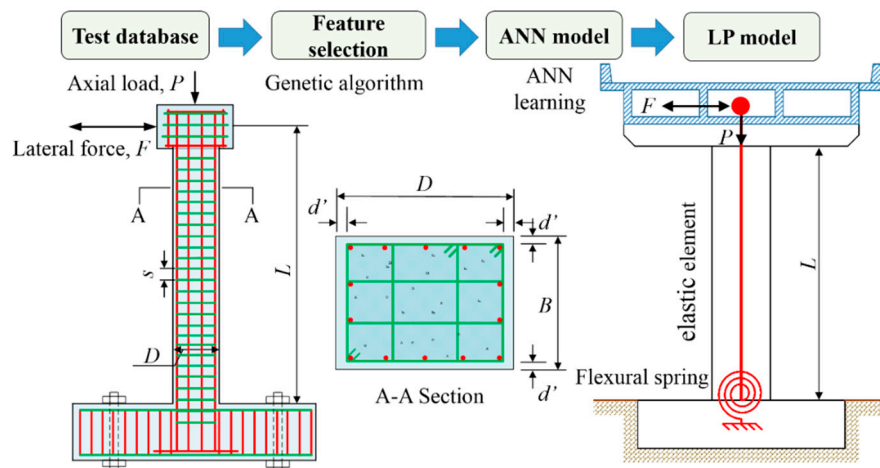


Figure 1. Schematic diagram and lumped plasticity model of a typical RC column.

As is known, there are many factors influencing the performance of RC columns, some of which are dependent. For example, the effective depth (d_e) can be calculated by B , D and the effective cover thickness (d'). Although the independent parameters are simple and easily accessible, the derived parameters may be more effective in some cases. Consequently, the potential influencing features are collected for feature selection, which are categorized into six groups as listed in Table 1. It can be observed from the table that a total of 24 features were included, in order to investigate their effects on RC columns.

Table 1. Features of reinforced concrete (RC) columns.

Category	Feature	Category	Feature
Cross Section	B	Long bars	ρ_l
	D		Longitudinal reinforcement ratio
	A_c		f_{yl}
	I_c		Yield strength of longitudinal bar
	d_e		f_{ul}
Span	L	Trans. bars	Ultimate strength of longitudinal bar
	λ		d_l
Vertical loading	P	Concrete	Diameter of longitudinal bar
	n		A_{sl}
Concrete	f'_c	Concrete	Area of a single longitudinal bar
	E_c		N_l
			Number of longitudinal bars
			f_{yt}
		Concrete	Yield strength of transverse steel
			f_{ut}
		Concrete	Ultimate strength of transverse steel
			d_{st}
		Concrete	Diameter of transverse reinforcement bar
			A_{st}
		Concrete	Area of one transverse reinforcement bar
			s
		Concrete	Spacing of transverse reinforcement
			ρ_{sv}
		Concrete	Transverse reinforcement volumetric ratio

As for the modeling, the LP model of RC columns is usually represented by the bi-linear and tri-linear model [28]. As shown in Figure 2, the strength and the yielding, capping and ultimate deformation of the RC columns can be defined according to the method using the hysteretic curves obtained from cyclic tests. The strength is defined as the peak point when the resistance force reaches its maximum value. According to statistical results by Haselton et al. [29], the yielding deformation can be roughly estimated as that corresponding to 85% of the peak strength, and the ultimate deformation is obtained from the drift when the resistance drops to 20% of the peak strength [6]. It should be noted that the actual test results of the hysteretic curve cannot always achieve perfect symmetry in both the positive and negative directions. Therefore, the mean values of the strength and deformation in the positive and negative directions were adopted for the following analysis. The strength and deformation capacities of 1163 RC columns were determined according to the above approach, and used as the outputs of the ANN model.

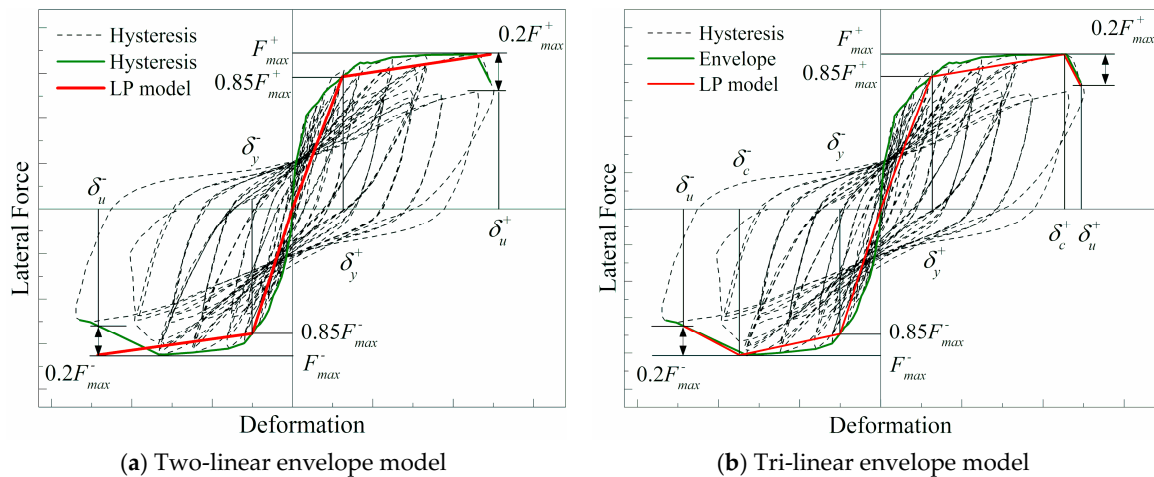


Figure 2. Schematic of hysteretic curves and definition of strength and deformation capacities.

Consequently, the model parameters of the LP model (e.g., yielding moment M_y , initial stiffness K_1 , and the coefficient of the post yielding stiffness r) can be determined by the four parameters: The strength (F_{max}), the yielding (δ_y), capping (δ_c) and ultimate drift (δ_u), as shown in Tables 2 and 3. As can be seen, $M_y = F_yL + P\delta_yL$ and $M_u = F_{max}L + P\delta_cL$ are the yielding moment and ultimate moment, respectively. Consequently, the four variables (F_{max} , δ_u , δ_c , δ_y) are used as the outputs of the ANN model.

Table 2. Definition and determination of the bi-linear lumped plasticity (LP) model.

Parameter	Description	Calculation
K_e	the initial stiffness of the linear segment	M_y / δ_y
M_y	the yielding moment	$F_yL + P\delta_yL$
b	the hardening ratio	$K_{sh} / K_e, K_{sh} = (M_c - M_y) / (\delta_u - \delta_y)$

Table 3. Definition and determination of the tri-linear LP model [30].

Parameter	Description	Calculation
K_e	the initial stiffness of the linear segment	M_y / δ_y
M_y	the yielding moment	$F_yL + P\delta_yL$
β_l	the pre-capping hardening ratio	$K_{sh} / K_e, K_{sh} = (M_c - M_y) / (\delta_c - \delta_y)$
β_c	the post-capping hardening ratio	$K_{ss} / K_e, K_{ss} = (M_c - M_u) / (\delta_u - \delta_c)$
M_c / M_y	the capping moment to the yielding moment	$M_c = F_{max}L + P\delta_cL, M_u = F_{max}L + P\delta_cL$

3. ANN Model

3.1. Architecture of the ANN Model

ANN is a humanlike information processing method, which is composed of many highly interconnected processing elements or neurons. In this study, the developed ANN model that maps the features of the RC column and the structural capacities can be written as:

$$y = f(x; \theta) \tag{1}$$

where y is the output feature vector of the ANN, including the strength and the yielding, capping and ultimate drift of the columns; x is the input feature vector of the column, as listed in Table 1; and θ represents the learning parameters.

As shown in Figure 3, a typical ANN architecture consists of an input layer, output layer and one or several hidden layers, and each layer has corresponding neurons [31]. In this study, back

propagation neural network (BPNN) [32] was adopted to predict the strength and deformation capacity of the columns. In the training process, the inputs propagate toward the output layer through the hidden layers, and errors between the predicted and experimental values back propagate from the output layer to the input layer to adjust the weights and thresholds of the hidden layers. In addition, the activation function defines how the input of a unit combines with its current activation level to complete a new activation. In this study, the commonly-used sigmoid activation function is utilized. Once the optimal connection weights and thresholds are determined, the trained ANN model can be conveniently employed to evaluate the strength and deformation capacities of RC columns.

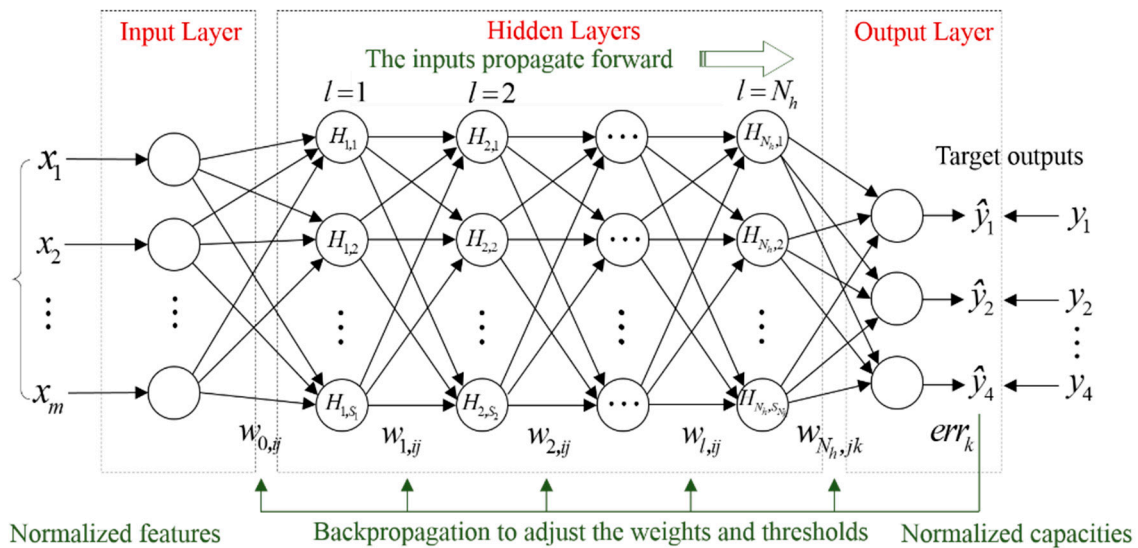


Figure 3. Architecture of the back propagation neural network (BPNN).

3.2. Input and Output Layer

As described previously, the strength and the deformation capacities of RC columns are affected by numerous factors. If all of the features are included in the input layer, the ANN model becomes very complex, and prone to fail due to overfitting. Therefore, it is reasonable to select an optimal input feature subset for the ANN model. To achieve optimization, all the input features listed in Table 1, and the output features are first organized into an $n \times m$ dimensional matrix and an $n \times 4$ dimensional matrix, respectively, as follows:

$$\mathbf{x} = \{x_{ij}\}_{n \times m}, \mathbf{y} = \{y_{ik}\}_{n \times 4} \quad (2)$$

where x_{ij} ($i = 1, 2, \dots, n$) is the j th input feature of the i th RC column in the training set, and y_{ik} ($k = 1, 2, 3, 4$) is the corresponding output feature of the i th RC column. Considering the significant difference in the value ranges of the features, data obtained from the specimens and the test results of the training set are first normalized within the range of $[0, 1]$ by:

$$\bar{x}_{ij} = \frac{x_{ij} - \min(\mathbf{x}_j)}{\max(\mathbf{x}_j) - \min(\mathbf{x}_j)}, \bar{y}_{ik} = \frac{y_{ik} - \min(\mathbf{y}_k)}{\max(\mathbf{y}_k) - \min(\mathbf{y}_k)} \quad (3)$$

where \bar{x}_{ij} is j th normalized input feature corresponding to the i th specimen; \mathbf{x}_j represents the j th input feature vector of all the specimens; and \mathbf{y}_k denotes the k th output feature vector. After normalization, n input–output pairs $\{\{\bar{\mathbf{x}}_i, \bar{\mathbf{y}}_i\}, i = 1, 2, \dots, n\}$ are collected into the training set, where $\bar{\mathbf{x}}_i = \{\bar{x}_{i1}, \bar{x}_{i2}, \dots, \bar{x}_{im}\}$ and $\bar{\mathbf{y}}_i = \{\bar{y}_{i1}, \bar{y}_{i2}, \dots, \bar{y}_{i4}\}$ are the normalized input and output features of the i th column, respectively.

In this study, a genetic algorithm (GA) was adopted to find the optimal input features of the column. GA is a metaheuristic inspired by the process of theoretical Darwinian natural selection in biological systems to generate high-quality solutions of search problems [33]. In this method, each

feature subset, such as structural configuration and material properties, is represented by an individual population. In the selection process, individuals with better phenotypic characteristics have greater probability to survive and reproduce in a population, whereas the less adapted individuals are more likely to disappear. Thus, the GA obtains the optimal solution after a series of iterative computations.

Figure 4 shows the chromosome design, fitness function and system architecture for the GA-based optimal feature selection of the columns, which operates in binary spaces (called chromosomes) and manipulates a population of potential solutions for the optimal input subset. A chromosome (genotype of the input features) is represented by binary coding as follows:

$$\boxed{g_1, g_2, \dots, g_j, \dots, g_m}, \quad g_j = \begin{cases} 1, & \text{if the } j\text{-th input feature is selected} \\ 0, & \text{if the } j\text{-th input feature is not selected} \end{cases} \quad (4)$$

where g_1, g_2, \dots, g_m represent the 24 input features that will be selected. The initial chromosome population is randomly generated first, using binary coding. For example, chromosome 100100 means that the first and the fourth input features were selected.

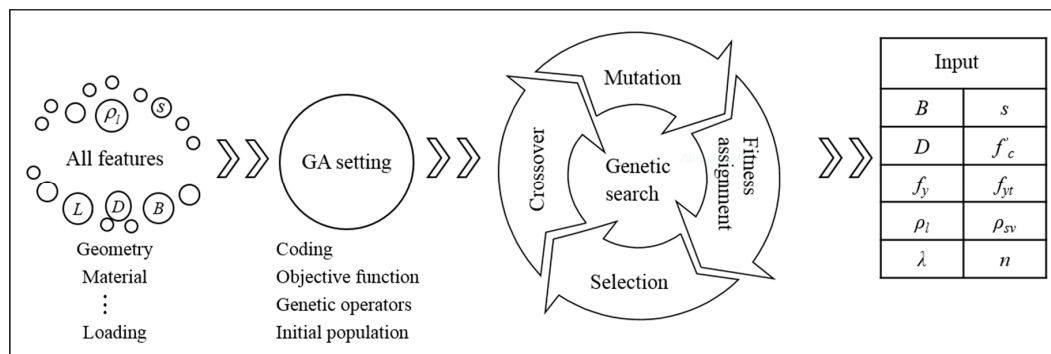


Figure 4. Genetic algorithm for optimal feature selection.

During the selection process, the fitness function is used to evaluate the quality of possible input subsets. There are several measurements can be used to evaluate the accuracy and survival probability of the chromosomes [34]. For convenience, the general fitness function is adopted in this study for the optimal input sets:

$$\text{fitness} = \frac{1}{\sum_{k=1}^4 \sum_{i=1}^n (\bar{y}_{ik} - \hat{y}_{ik})^2} \quad (5)$$

where \bar{y}_{ik} and \hat{y}_{ik} are the k th experimental result and predicted value of the i th specimen, respectively. For the selection of the optimal input features, an ANN model with one hidden layer containing 20 neurons is used, as the optimal ANN architecture is still not obtained in this stage.

Fitter chromosomes from the current population have a higher probability to be selected to generate offspring population using genetic operators, namely crossover and mutation. The population size, number of generations, crossover rate and mutation rate of the GA were selected as 500, 25, 0.8, and 0.3, respectively, using the approach proposed by Oliveira et al. [35]. This evaluation process will be performed iteratively until the termination criterion (10^{-3}) is satisfied. After that, the most fitted features can be determined as the inputs for ANN training.

The optimal input feature subset with 10 nodes, including $B, D, f'_c, f_{yl}, \lambda, f_{yt}, s, \rho_l, \rho_{sv}$ and n were selected from the 24 features listed in Table 1 using GA. Laboratory test results reported by [36] also demonstrate that the selected optimal features are the most important parameters that affect the seismic performance of these RC columns. However, other parameters, like the effective cover thickness (d') and depth (d_e), may be also important. The reason for omitting them is that they are either similar in most specimens, or can be easily calculated. For example, the d' of most of the specimens is in the range of 0.02 m to 0.03 m, while the d_e can be determined based on B and d' .

4. Results and Discussion

4.1. Training of the ANN Model

Before training the ANN model, all of the collected structural and material parameters of the 1163 specimens and the corresponding test results on the strength and drift capacities were normalized as the input and output vectors using the above approach. Then, 863 specimens in the database were randomly selected as the training set ($n_{train} = 863$). While the remaining specimens were used as the test set ($n_{test} = 150$) and validation set ($n_{validation} = 150$), respectively.

The number of input and output nodes in the ANN architecture is obviously 10 and 4, respectively. The following parameters of the BPNN were used in training the model: (1) Error tolerance = 10^{-3} ; (2) learning parameter = 0.15; (3) maximum number of iterations = 10^4 ; (4) momentum parameter = 0.05; (5) noise = 0.01. The mean absolute error (E) and goodness of fit (R^2) were adopted to evaluate the accuracy of the ANN model, as follows:

$$E_k = \frac{1}{N} \sum_{i=1}^N \left| \frac{\bar{y}_{ik} - \hat{y}_{ik}}{\bar{y}_{ik}} \right|, \quad (k = 1, 2, \dots, 4) \tag{6}$$

$$R_k^2 = 1 - \frac{\sum_{i=1}^N (\bar{y}_{ik} - \hat{y}_{ik})^2}{\sum_{i=1}^N (\bar{y}_{ik})^2}, \quad (k = 1, 2, \dots, 4) \tag{7}$$

where N is the number of specimens in the training set or test and validation set.

It should be noted that there is no specific rule or heuristics [37] to determine the number of hidden layers and the corresponding number of nodes. In general, an ANN model with too many neurons tends to fail due to an overfitting of the training data, whereas those with few neurons may not be able to capture the complex underlying relationship. Therefore, several trials were conducted for ANN models with different nodes and a single hidden layer to obtain an optimal ANN architecture for the strength and deformation capacity prediction of RC columns. For an optimal ANN architecture, the mean absolute error and goodness of fit of the ANN model should satisfy the following criteria: (1) Well-distributed around 0 (smaller E_k) and (2) as close as possible (larger R_k^2). The mean value ($E = \bar{E}_k, R^2 = \bar{R}_k^2$) of the four properties was used.

Figure 5 shows the test results of the trained ANN models with 10–50 hidden neurons. It can be observed that the mean absolute error and goodness of fit of the three properties are within the range of [0.126, 0.142] and [0.870, 0.882], respectively. As can be seen, the N-10-21-4 ANN architecture has the smallest E and largest R^2 , and thus was determined as the optimal ANN architecture.

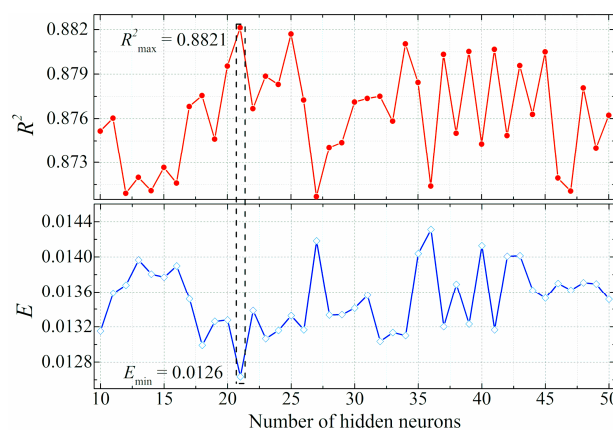


Figure 5. Comparison of artificial neural network (ANN) architectures.

4.2. Validation

Experimental data in the training set, test set and validation set were used to validate the ANN model. Figure 6 shows a comparison of the predicted strength capacities by the ANN model and the experiments. It can be observed that the predicted values of the strength are in good agreement with the experimental values of the columns. For the normalized strength, the mean absolute error and goodness of fit are 0.0533 and 0.9304, respectively, for the training set, and 0.0133 and 0.9431, respectively, for the test and validation set. The results indicate that the ANN model can be effectively used to predict the strength of the RC columns under seismic excitations.

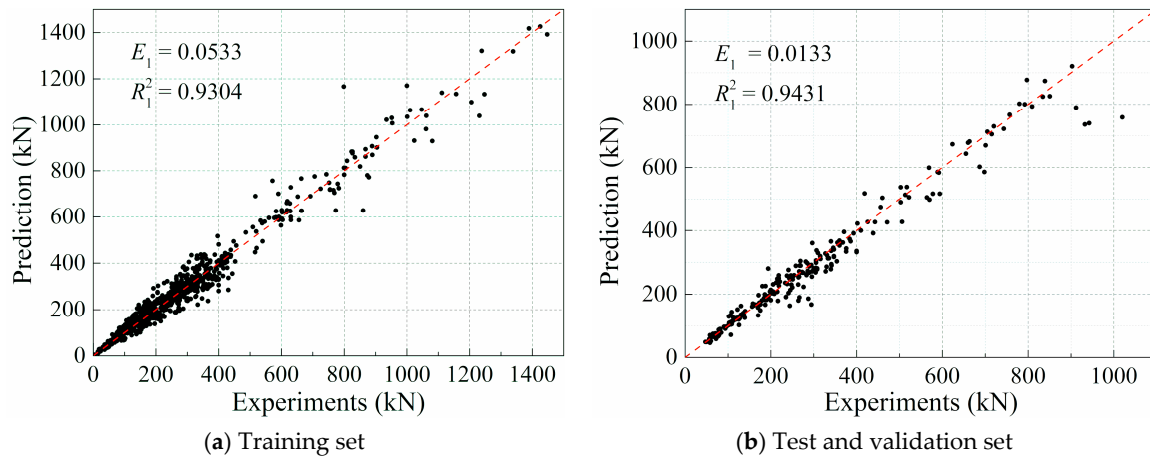


Figure 6. Comparison of experimental results and predicted results of the strength of RC columns.

Different types of explicit formulas have been proposed by researchers or adopted in design codes for calculating the strength of RC columns. In general, concrete and reinforcement contribute to the shear capacity of RC columns with shear failure mode. Therefore, the explicit formula has two distinct parts.

$$V = V_c + V_s \tag{8}$$

where $V = F_{max}$ is the shear strength for shear-failed columns, while V_c and V_s are the contributions of concrete and steel reinforcement, respectively. In this study, three types of explicit formulas for predicting the shear strength of RC columns were adopted to validate the ANN model as summarized in Table 4.

Table 4. Explicit formulas for estimating the shear capacity of RC columns.

Reference	Concrete Contribution (V_c)	Steel Contribution (V_s)
Sezen and Moehle [5] FEMA 356 [3]	$V_c = k_\mu \left(\frac{0.5\sqrt{f'_c}}{\lambda} \sqrt{1 + \frac{P}{0.5\sqrt{f'_c}A_c}} \right) 0.8A_c$	$V_s = k_\mu \frac{A_{st}f_{yt}D'}{s}$
ACI 318-05 [38]	$V_c = \frac{1}{6} \left(1 + \frac{P}{13.8A_c} \right) \sqrt{f'_c}A_c$	$V_s = \frac{A_h f_{yh} D'}{s}$
FEMA 273 [39]	$V_c = 0.29\lambda \left(k + \frac{P}{13.8A_c} \right) \sqrt{f'_c}A_c$	$V_s = \frac{A_{st}f_{yt}D'}{s}$

Note: k_μ is the ductility-related strength degradation factor, and D' is the distance from the extreme compression fiber to the centroid of the tension reinforcement. The meanings of other parameters in this table are the same as those in Table 1.

For flexural-dominated specimens, the lateral loading capacity is strongly dependent on the flexural strength (M_c) and the distance between the critical section of the plastic hinge and point of contra-flexure length (L), as follows:

$$F_{max} = (M_c - P \cdot \Delta_c) / L = (M_y \cdot M_c / M_y - P \cdot \Delta_c) / L \tag{9}$$

where Δ_c is the capping displacement corresponding to the maximum lateral strength (F_{max}). Fardis et al. [40] proposed a semi-empirical strength and deformation expression with good average agreement with test results. It has been widely used in the seismic performance assessment in engineering [29]

$$M_c/M_y = (1.25)(0.89)^n(0.91)^{0.01f'_c} \tag{10}$$

$$M_y = BD^3\phi_y \left\{ E_c \frac{k_y^2}{2} \left[0.5(1 + \delta') - \frac{k_y}{3} \right] + \frac{E_s}{2} \left[(1 - k_y)\rho + (k_y - \delta')\rho' + \frac{\rho_v}{6}(1 - \delta') \right] (1 - \delta') \right\} \tag{11}$$

where ϕ_y is the yield curvature; δ' is the ratio of the distance of the compression reinforcement center from the extreme compression fibers to the span depth (D); k_y is the normalized compression zone depth; E_s is the reinforcement elastic modulus; ρ , ρ' and ρ_v are the reinforcement ratios of tension, compression and web reinforcement, respectively.

Figure 7 shows a comparison of the experimental results, predicted strength of the ANN model and calculated results from the explicit formula. In Figure 7a, the test results of the shear-failed specimens were obtained using the formula by [5], while the flexural failure specimens were selected from the database of this study. As shown in Figure 7a, the mean absolute error of the predicted shear strength of the ANN model is 0.107, which is smaller than those obtained from the three explicit formulas, 0.235, 0.207 and 0.217. In Figure 7b, it can also be observed that the mean absolute error of the ANN model is 0.087. However, the statistical result of the mean absolute error obtained from the design code is 0.101. It is illustrated that the results indicate that the ANN model yields a more accurate prediction of the structural strength of the columns.

Figure 8 also shows a comparison of the test results of the ultimate drift of the column, and predicted results from the ANN model. It can be observed that the ANN model can also achieve a reasonable prediction of the ultimate drift. However, it is evident that the mean absolute error of the ultimate drift is larger than that of the strength prediction, particularly for specimens with large ultimate deformation capacity.

The mean absolute error and goodness of fit are found to be 0.1761 and 0.8114, respectively, for the training set, and 0.1783 and 0.8216 for the test and validation set, respectively. This is because the ultimate deformation of the column is more strongly affected by the nonlinearity of the structures. Another reason for there being less accuracy is that the ultimate deformation is more difficult to measure.

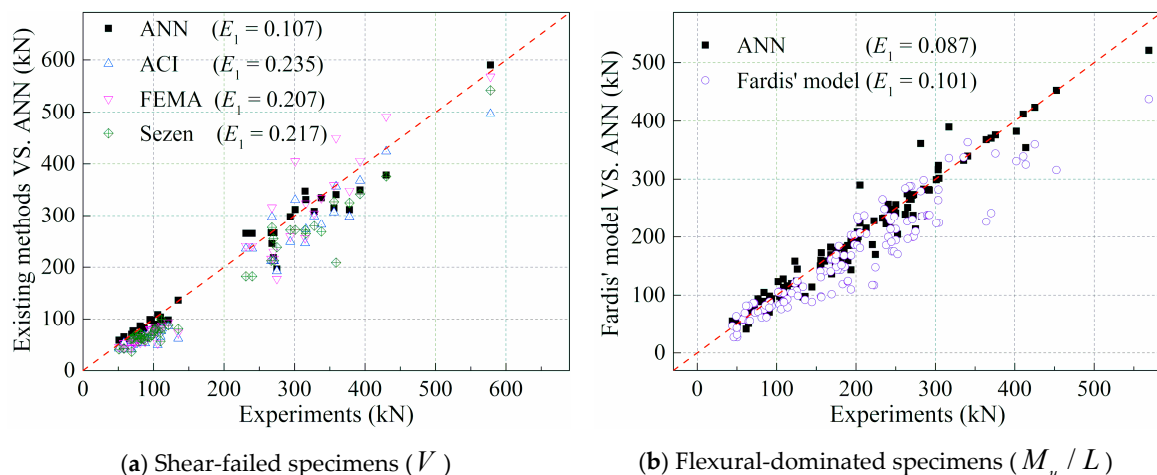


Figure 7. Comparison of the predicted results of the strength from the ANN model and existing explicit formulas.

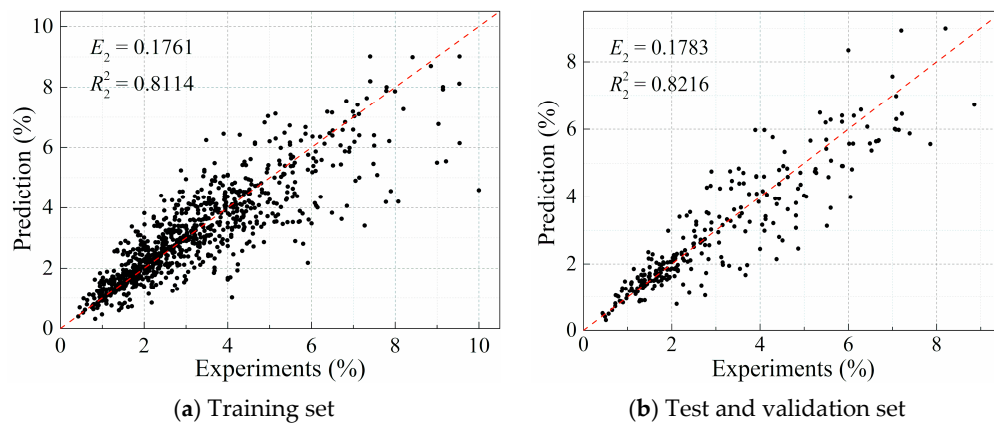


Figure 8. Comparison of experimental results of the ultimate drift and predicted results from the ANN model.

To assess the ultimate deformation of lightly reinforced columns, Elwood et al. [6] proposed an explicit formula given as follows:

$$\frac{\Delta_u}{L} = \frac{3}{100} + 4\rho_t - \frac{1}{40} \frac{F_{max}}{A_c \sqrt{f'_c}} - \frac{n}{40} \geq 1\%(\text{MPa}) \tag{12}$$

where the effects of the transverse reinforcement ratio (ρ_t), axial load ratio (n) and strength (F_{max}) are taken into account. Furthermore, Lehman et al. [41] also developed an explicit method to evaluate the ultimate drift of flexural-dominated columns as follows:

$$\frac{\Delta_u}{L} = \frac{\Delta_y}{L} + \frac{\Delta_{sp}}{L} + \frac{\Delta_f}{L} \tag{13}$$

where Δ_y , Δ_{sp} and Δ_f are the yield, slip and flexural displacement, respectively.

The above explicit formulas for calculating the ultimate drift were also used to validate the accuracy and effectiveness of the ANN model. Figure 9 shows a comparison of results obtained from the formula methods and test results from the collected test database, which are divided into two parts, namely the shear-failed specimens and the flexural-dominated specimens. It can be observed that the ANN model also yields better prediction of the ultimate drift than the two explicit formulas. The mean absolute errors obtained from the ANN model and the Elwood’s method are 0.165 and 0.266, respectively, for the shear-failure columns, whereas those obtained from the ANN model and the Lehman’s method are 0.188 and 0.316, respectively, for the flexural-failure columns.

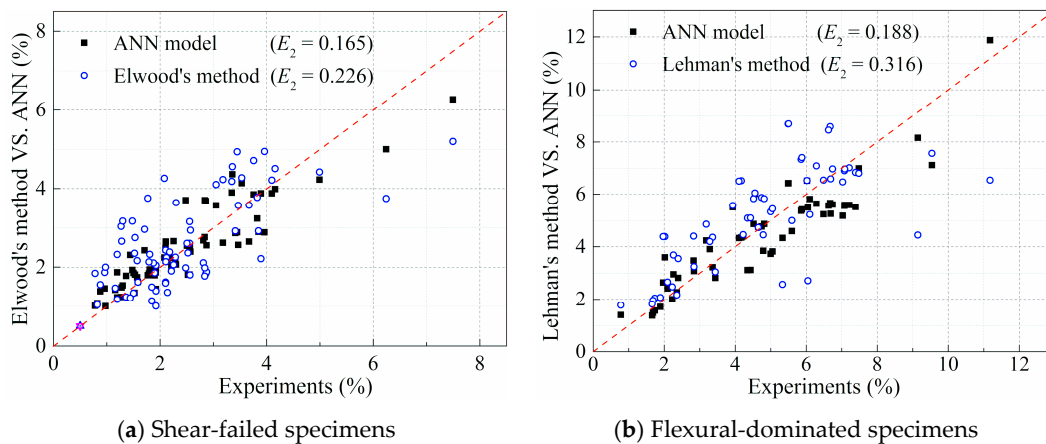


Figure 9. Comparison results of the ultimate drift between the experimental, ANN model and explicit methods.

Since there are currently no explicit formula for the estimation of capping drift corresponding to the maximum strength, Figure 10 only shows the comparison of the experimental results of the capping drift of the column and the predicted results from the ANN model, with the mean absolute error of 0.0794 and 0.1071, goodness of fit of 0.8001 and 0.8345, for the training set and the test and validation set, respectively. Nevertheless, it can still be seen that the ANN-based model for the capping drift estimation is reasonable and relatively accurate.

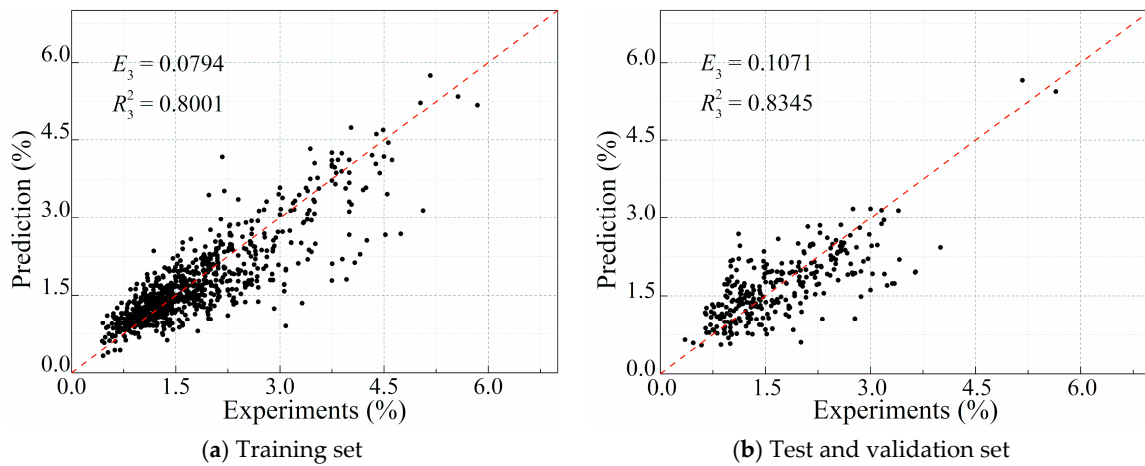


Figure 10. Comparison of experimental results of the capping drift and predicted results from the ANN model.

Similarly, Figure 11 shows a comparison of the yielding drift of column between experimental results and predicted results from the ANN model. The mean absolute error for the training set and the test-validation set is 0.1081 and 0.0752, and the corresponding goodness of fit is 0.8548 and 0.8638, respectively. Generally, the yielding drift of RC columns always appears earlier with low nonlinearity than the ultimate drift. Therefore, the proposed ANN-based model can get a better prediction on the yielding drifts than the ultimate drift due to the nonlinearity difference between these two physical parameters.

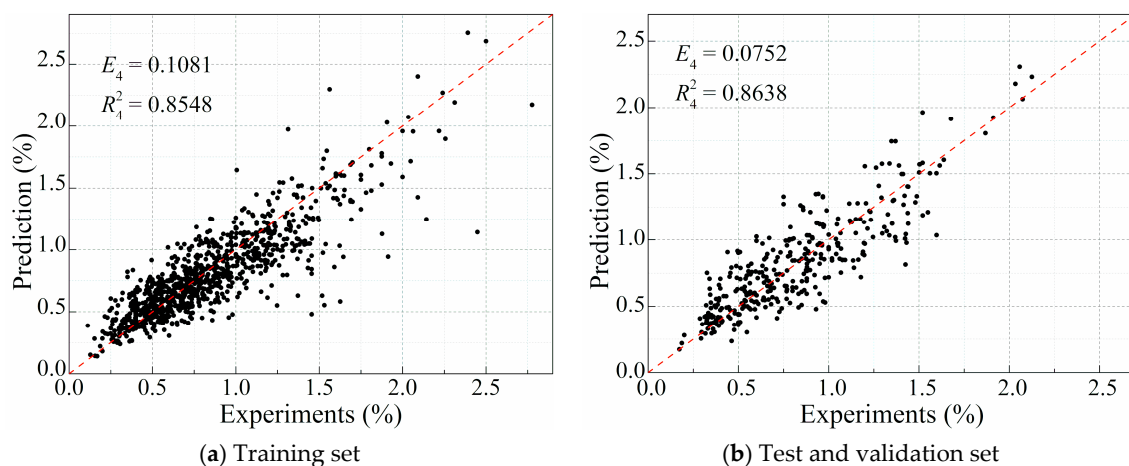


Figure 11. Comparison of experimental results of the yielding drifts and predicted results from the ANN model.

For the estimation of the yielding drift, Fardis et al. [40] proposed a statistical formula based on the results of 963 tests, which has been widely used in engineering [29].

$$\delta_y = \phi_y \frac{L}{3} + 0.0025 + \alpha_{sl} \frac{0.25 \varepsilon_y d_l f_{yl}}{(d - d') \sqrt{f'_c}} \tag{14}$$

where ϕ_y is the yielding curvature of the section, α_{sl} is the slip coefficient (equals 1 if slippage of longitudinal steel is possible, or 0 if it is not), and ε_y is the yield strain of longitudinal steel.

Figure 12 presents the comparison results of the yielding drift estimation of RC columns from the test set between the proposed ANN model and Fardis' method. It shows that the ANN model performs better than the empirical formula, with the mean absolute error of 0.2327 and 0.4572, respectively. Therefore, the developed ANN-based model can provide a more reliable and accurate prediction of the critical parameters for the LP model.

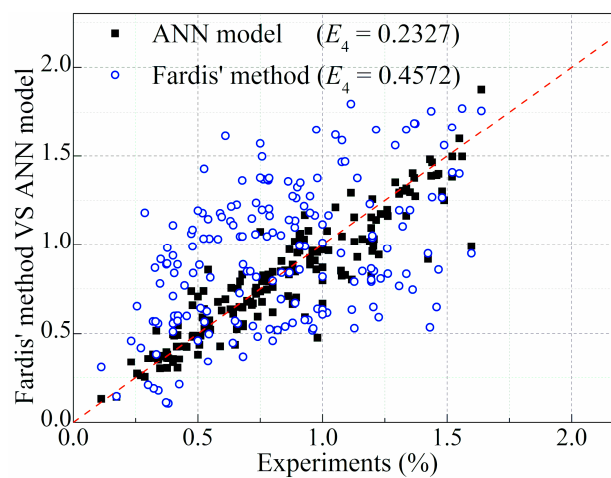


Figure 12. Comparison results of the yield drift between the experimental, ANN model and Fardis' method [40].

4.3. Evaluation of the ANN-Based LP Model

4.3.1. Comparison with the Pseudo-Static Test

The boundary conditions of the RC column during pseudo-static tests are generally close to its real situation. Therefore, it is reasonable to validate the ANN-based bi-linear and tri-linear LP model through a quasi-stable test on a frame. This test was conducted by [42], and the simulation is carried out using the Open System for Earthquake Engineering Simulation (OpenSEES, [28]) platform, as shown in Figure 13a. Each column was simulated by one elastic element and two zero-length elements at the two ends, as shown in Table 5. As illustrated in Figure 13b, the ANN-based LP model can provide an acceptable prediction result, especially for the envelope curve. It also shows that the ANN-based tri-linear model performs better than the bi-linear one during the whole hysteresis curve prediction process, especially after the capping point.

Table 5. ANN-based method for the LP model of the RC column sample [42].

Model	Parameters
ANN model	$F_{max} = 27.50 \text{ kN}$, $\delta_u = 4.53\%$, $\delta_c = 1.85\%$, $\delta_y = 1.17\%$
Bi-linear model	$K_e = 1119 \text{ kN}\cdot\text{m/rad}$, $M_y = 13.09 \text{ kN}\cdot\text{m}$, $b = 0.061$
Tri-linear model	$K_e = 1119 \text{ kN}\cdot\text{m/rad}$, $M_y = 13.09 \text{ kN}\cdot\text{m}$, $\beta_l = 0.18$, $\beta_c = -0.128$, $M_c/M_y = 1.17$

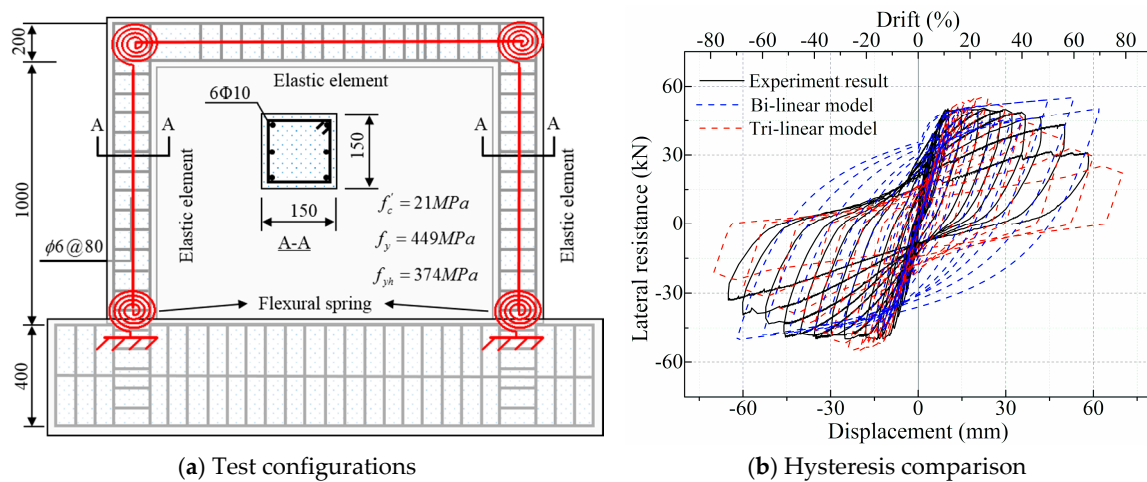


Figure 13. Comparison of the ANN-based LP model and test result [42].

4.3.2. Comparison with Shake Table Test

For further validation, a time history response comparison was performed between the proposed ANN-based method and a shaking table test of a single-story RC frame [43]. As shown in Figure 14, the frame consists of two identical columns and a rigid link beam. Each column is modeled by one elastic element and two flexural springs at the two ends. Based on their properties, the ANN model was used to predict their strength and deformation capacities, as presented in Table 6. Therefore, the parameters for bilinear model (M_y, K_e, b) and tri-linear model parameters ($K_e, M_y, \beta_l, \beta_c, M_c / M_y$) of their LP models were calculated, based on which the FE model was developed on the OpenSEES platform.

During the test, the structure was subjected to a scaled ground motion with $PGA = 1.28\text{ g}$ (recorded by TCU076NS in the 1999 Chi-Chi earthquake), as shown in Figure 15a. After performing the dynamic time history analysis, the drift response of the specimen was obtained and compared with the test result, as is shown in Figure 15b. It is observed that the ANN-based LP models can provide an acceptable estimation of the drift response before the collapse of the frame structure, especially for the tri-linear one. The corresponding maximum error of the drift response before the time of 22.6 s between the ANN-based tri-linear model and the test is very small. However, due to the limitation of the LP model itself, the collapse phenomenon of the specimen could not have been directly represented during the simulation. In spite of that, the proposed ANN-based model-free and data-driven method is still an effective and reliable candidate for the researchers and engineers to determine the key parameters of RC columns during finite element analysis.

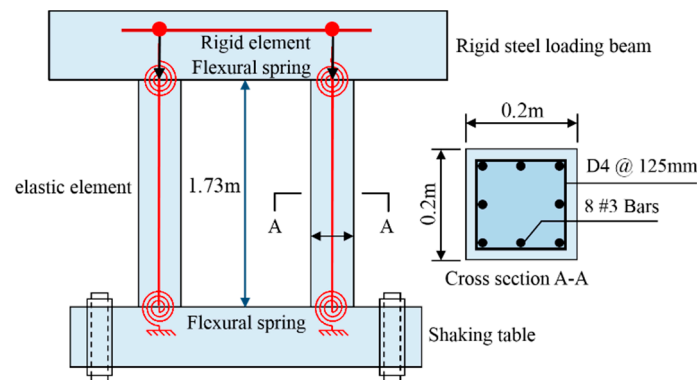
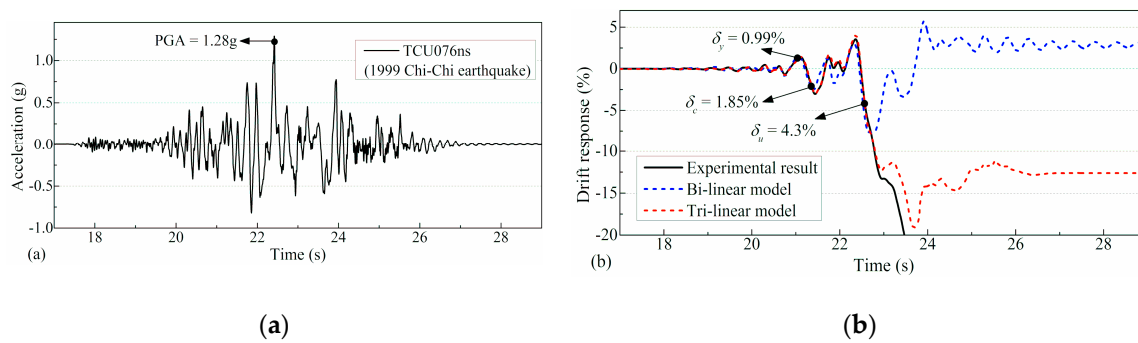


Figure 14. Prototype and model of the shaking table specimen.

Table 6. ANN-based method for the LP model of RC column sample S2 [43].

Model	Parameters
ANN model	$F_{\max} = 36.62 \text{ kN}$, $\delta_u = 4.53\%$, $\delta_c = 1.85\%$, $\delta_y = 0.99\%$
Bi-linear model	$K_e = 2720 \text{ kN}\cdot\text{m}/\text{rad}$, $M_y = 26.92 \text{ kN}\cdot\text{m}$, $b = 0.0494$
Tri-linear model	$K_e = 2720 \text{ kN}\cdot\text{m}/\text{rad}$, $M_y = 26.92 \text{ kN}\cdot\text{m}$, $\beta_l = 0.203$, $\beta_c = -0.087$, $M_c/M_y = 1.17$

**Figure 15.** Drift response comparison of the frame obtained from test and ANN-based LP model: (a) Ground motion record; and (b) drift response.

The developed ANN-based model for the LP parameters of RC columns has been already implemented in an efficient Matlab GUI, anyone has access to it in the supplementary materials.

5. Conclusions

This study explored the possibility of using an ANN-based method to rapidly determine the seismic performance of RC columns, as well as the development of the LP model for them. An ANN model was established and validated based on the large database of 1163 cyclic tests of RC columns to predict the strength and the yielding, capping and ultimate deformation capacities, which are critical for the commonly-used LP model. The following conclusions are drawn:

1. On the basis of a large historical experimental database and advanced humanlike information processing algorithm, the proposed model-free method in this study can rapidly get more accurate input parameters for any bilinear and tri-linear LP model than current explicit formulas. The accuracy of the proposed method can also have been improved with the increment of the sample quantity of the database.
2. The validation results through both the collected experimental data and several existing functions indicate that the ANN-based method can be effectively used to predict the most important characteristics of RC columns, which are also critical for the further modeling of structures. In addition, another advantage of the proposed model-free method is that the quantity of the input features could be easily changed according to the requirement of an arbitrary multi-linear model.
3. The ANN-based LP model can help reduce the subjective and experimental errors. The prediction results of the RC frame structures using the well-trained ANN-based LP model show a good agreement with both the quasi-static and shaking table test results, especially for the pre-collapse stage. Thus, the model-free method based on the machine learning theory will be an innovative and promising approach for a fast seismic performance evaluation of the buildings and bridges in the future.

Thus, the model-free method based on the machine learning theory (e.g., ANN method) can be used as a promising surrogate for the rapid seismic performance evaluation of the buildings and bridges in the future.

Supplementary Materials: The well-trained ANN-based model for the LP parameters of RC columns has been already implemented in an efficient Matlab GUI, which is available for the users, including both of the researchers and engineers to quickly evaluate the seismic performance of RC columns as well as RC structures. Anyone who is interested in the ANN-based LP model of RC column in this study may contact the author or download the program from the following address: <https://www.dropbox.com/s/8aq3qreiochn26o/ANNLPGUI.zip?dl=0>.

Author Contributions: Z.L. collected the test database, developed the ANN model and wrote the manuscript. S.L. contributed to the idea of the study, modified the computer program and supervised and verified the manuscript.

Funding: This research was funded by the National Key Research and Development Program of China (2018YFC0809404 and 2016YFC0701107) and the National Natural Science Foundation of China (51725801).

Conflicts of Interest: The authors declare no conflict of interest.

Appendix A

Table A1. Details of specimens included in the database.

References	Number of Specimens	Width (mm)	Shear Span (mm)	Concrete Strength (MPa)	Axial Load Ratio
Berry and Eberhard [44]	132	150–550	160–2200	16–160	0.0–0.8
Browning et al. [26]	168	80–800	80–2500	13–116	0.0–0.9
Yun [45]	6	510	1778	62.1–64.1	0.20–0.34
Ho and Johnny [46]	20	325	1515	56.5–111.1	0.11–0.55
Ongsupankul et al. [47]	4	400	1550	29.61–32.36	0.07–0.08
Woodward and Jirsa [48]	5	300	455	31–41	0.0–0.21
Bayrak [49]	24	250–350	1473	70.8–112.1	0.31–0.53
Mo and Wang [50]	9	400	1400	24.9–27.5	0.1–0.21
Paultre et al. [51]	8	305	2150	78.7–110	0.35–0.53
Xiao and Yun [52]	6	510	1778	62.1, 64.1	0.2–0.34
Lam et al. [53]	9	160–267	400–480	42, 47	0.4–0.65
Hwang and Yun [54]	8	200	300	68.3–70.3	0.3
Moretti and Tassios [7]	8	250	250–750	35–49	0.3, 0.6
Ahn and Shin [55]	20	240	500	32–70	0.3–0.5
Woods et al. [56]	7	203	625	69	0.16
Marefat et al. [57]	7	150–200	750	20–28	0.16–0.31
Xiao et al. [58]	6	200	850	60, 90	0.38–0.54
Bae [59]	5	610, 440	2630	29.6–43.4	0.2, 0.5
Cao [60]	10	250, 350	600, 850	22.6–32.5	0.2–0.5
Ou et al. [61]	8	600	900	92.5–121	0.1, 0.2
Abdelsamie et al. [62]	7	250	700, 1050	26.6–151.4	0
Martirosyan and Xiao [63]	6	254	508	76, 86	0.1, 0.2
Li et al. [64]	8	300	250–500	23.4–27.5	0.09–0.29
Nakamura et al. [65]	6	450	450, 700	25, 28	0.16–0.18
Popa et al. [66]	7	300	450	18–29	0.2–0.4
Jin et al. [67]	8	150	495–660	34–73	0.09, 0.13
Bechtoula et al. [68]	10	325–520	813–1300	80, 130	0.3
El-Attar et al. [69]	7	150	870	141	0–0.35
Personal communications	626	150–900	150–3500	20–180	0–0.9

References

- Guo, A.; Liu, Z.; Li, S.; Li, H. Seismic performance assessment of highway bridge networks considering post-disaster traffic demand of a transportation system in emergency conditions. *Struct. Infrastruct. Eng.* **2017**, *13*, 1523–1537. [CrossRef]
- Eurocode 8: Design of Structures for Earthquake Resistance—Part 3: Assessment and Retrofitting of Buildings*; European Committee for Standardization: Brussels, Belgium, 2005.
- American Society of Civil Engineers. *Prestandard and Commentary for the Seismic Rehabilitation of Buildings*; FEMA 356: Washington, DC, USA, 2000.

4. Priestley, M.N.; Verma, R.; Xiao, Y. Seismic shear strength of reinforced concrete columns. *J. Struct. Eng.* **1994**, *120*, 2310–2329. [[CrossRef](#)]
5. Sezen, H.; Moehle, J.P. Shear Strength Model for Lightly Reinforced Concrete Columns. *J. Struct. Eng.* **2004**, *130*, 1692–1703. [[CrossRef](#)]
6. Elwood, K.J.; Moehle, J.P. Drift Capacity of Reinforced Concrete Columns with Light Transverse Reinforcement. *Earthq. Spectra* **2005**, *21*, 71–89. [[CrossRef](#)]
7. Moretti, M.; Tassios, T.P. Behaviour of short columns subjected to cyclic shear displacements: Experimental results. *Eng. Struct.* **2007**, *29*, 2018–2029. [[CrossRef](#)]
8. Taheri, A.; Moghadam, A.S.; Tasnimi, A.A. Critical factors in displacement ductility assessment of high-strength concrete columns. *Int. J. Adv. Struct. Eng.* **2017**, *9*, 325–340. [[CrossRef](#)]
9. Mostafaei, H.; Vecchio, F.J.; Kabeyasawa, T. Deformation Capacity of Reinforced Concrete Columns. *ACI Struct. J.* **2009**, *106*, 187–195.
10. Wibowo, A.; Wilson, J.L.; Lam, N.T.K.; Gad, E.F. Drift Capacity of Lightly Reinforced Concrete Columns. *Aust. J. Struct. Eng.* **2011**, *15*, 131–150. [[CrossRef](#)]
11. Ferdous, W.; Manalo, A.; Aravinthan, T.; Fam, A. Flexural and shear behaviour of layered sandwich beams. *Const. Build. Mater.* **2018**, *173*, 429–442. [[CrossRef](#)]
12. Ferdous, W.; Manalo, A.; Erp, G.V.; Aravinthan, T.; Ghabraie, K. Evaluation of an Innovative Composite Railway Sleeper for a Narrow-Gauge Track under Static Load. *J. Compos. Const.* **2018**, *22*, 04017050. [[CrossRef](#)]
13. Kim, S.-H.; Han, S.-J.; Kim, K.S. Nonlinear Finite Element Analysis Formulation for Shear in Reinforced Concrete Beams. *Appl. Sci.* **2019**, *9*, 3503. [[CrossRef](#)]
14. Szcześniak, A.; Stolarski, A. Dynamic Relaxation Method for Load Capacity Analysis of Reinforced Concrete Elements. *Appl. Sci.* **2018**, *8*, 396. [[CrossRef](#)]
15. Lucchini, A.; Franchin, P.; Kunnath, S. Failure simulation of shear-critical RC columns with non-ductile detailing under lateral load. *Earthq. Eng. Struct. Dyn.* **2017**, *46*, 855–874. [[CrossRef](#)]
16. Lu, X.; Ye, L.; Pan, P.; Zhao, Z.; Ji, X.; Qian, J. Pseudo-static collapse experiments and numerical prediction competition of RC frame structure I: RC frame experiment. *Build. Struct.* **2012**, *42*, 23–26.
17. Ibarra, L.F.; Medina, R.A.; Krawinkler, H. Hysteretic models that incorporate strength and stiffness deterioration. *Earthq. Eng. Struct. Dyn.* **2005**, *34*, 1489–1511. [[CrossRef](#)]
18. Haselton, C.B.; Liel, A.B.; Deierlein, G.G. Simulation structural collapse due to earthquakes: Model calibration, and numerical solution algorithms. In Proceedings of the Computational Methods in Structural Dynamics and Earthquake Engineering (COMPDYN), Rhodes, Greece, 22–24 June 2009.
19. Liel Abbie, B.; Haselton Curt, B.; Deierlein Gregory, G. Seismic Collapse Safety of Reinforced Concrete Buildings. II: Comparative Assessment of Nonductile and Ductile Moment Frames. *J. Struct. Eng.* **2011**, *137*, 492–502. [[CrossRef](#)]
20. Lucchi, E. Non-invasive method for investigating energy and environmental performances in existing buildings. In Proceedings of the PLEA—Architecture and Sustainable Development, Louvain-la-Neuve, Belgium, 13–15 July 2011.
21. Kawashima, K.; Oreta, A.W.C. Neural Network Modeling of Confined Compressive Strength and Strain of Circular Concrete Columns. *J. Struct. Eng.* **2003**, *129*, 554–561.
22. Iztok, P.; Karmen, P.; Fajfar, P. Flexural deformation capacity of rectangular RC columns determined by the CAE method. *Earthq. Eng. Struct. Dyn.* **2006**, *35*, 1453–1470.
23. Chou, J.-S.; Ngo, N.-T.; Pham, A.-D. Shear Strength Prediction in Reinforced Concrete Deep Beams Using Nature-Inspired Metaheuristic Support Vector Regression. *J. Comput. Civ. Eng.* **2016**, *30*, 04015002. [[CrossRef](#)]
24. González, M.P.; Zapico, J.L. Seismic damage identification in buildings using neural networks and modal data. *Comput. Struct.* **2008**, *86*, 416–426. [[CrossRef](#)]
25. Reza, S.M.; Alam, M.S.; Tesfamariam, S. Lateral load resistance of bridge piers under flexure and shear using factorial analysis. *Eng. Struct.* **2014**, *59*, 821–835. [[CrossRef](#)]
26. Browning, J.A.; Pujol, S.; Eigenmann, R.; Ramirez, J.A. NEEShub Databases. *Concrete International*. 2013, Volume 35. Available online: <https://datacenterhub.org/resources/databases> (accessed on 4 April 2013).
27. University of Washington. The UW-PEER Reinforced Concrete Column Test Database. Available online: [http://www.ce.washington.edu/~sim\\$peera1/](http://www.ce.washington.edu/~sim$peera1/): (accessed on 1 January 2004).

28. Mckenna, F.; Fenves, G.L. Open system for earthquake engineering simulation (OpenSees). In *Pacific Earthquake Engineering Research Center*; University of California: California, CA, USA, 2013.
29. Haselton, C.B. *Beam-Column Element Model Calibrated for Predicting Flexural Response Leading to Global Collapse of RC Frame Buildings*; Pacific Earthquake Engineering Research Center: Berkeley, CA, USA, 2008.
30. Dimitrios, L. *Sidesway Collapse of Deteriorating Structural Systems under Seismic Excitations*; Stanford University: Stanford, CA, USA, 2009.
31. Ziegel, E.R. *The Elements of Statistical Learning*; World Publishing Corporation: New York, NY, USA, 2015.
32. Flood, I. *Neural networks in civil engineering: A review. Civil and Structural Engineering Computing*; Saxe-Coburg Publications: Stirling, UK, 2001; pp. 185–209.
33. Booker, L.B.; Goldberg, D.E.; Holland, J.H. Classifier systems and genetic algorithms. *Artif. Intell.* **1989**, *40*, 235–282. [[CrossRef](#)]
34. Shafti, L.S.; Pérez, E. Fitness Function Comparison for GA-Based Feature Construction. In *Proceedings of the Current Topics in Artificial Intelligence, Conference of the Spanish Association for Artificial Intelligence, Caepia, Salamanca, Spain, 12–16 November 2007*; pp. 249–258.
35. Oliveira, A.L.I.; Braga, P.L.; Lima, R.M.F.; Lio, M.; Rcio, L. GA-based method for feature selection and parameters optimization for machine learning regression applied to software effort estimation. *Inf. Softw. Technol.* **2010**, *52*, 1155–1166. [[CrossRef](#)]
36. Li, D.; Jin, L.; Du, X.; Fu, J.; Lu, A. Size effect tests of normal-strength and high-strength RC columns subjected to axial compressive loading. *Eng. Struct.* **2016**, *109*, 43–60. [[CrossRef](#)]
37. Zhang, G.; Patuwo, B.E.; Hu, M.Y. Forecasting with artificial neural networks: The state of the art. *Int. J. Forecast.* **1998**, *14*, 35–62. [[CrossRef](#)]
38. ACI 318-05. *Building Code Requirements for Structural Concrete*; Farmington Hills: Oakland, MI, USA, 2002; pp. 16–17.
39. FEMA, F. *NEHRP Guidelines for the Seismic Rehabilitation of Buildings: FEMA 273*; Federal Emergency Management Agency: Washington, DC, USA, 1997.
40. Telemachos, B.P.; Michael, N.F. Deformations of Reinforced Concrete Members at Yielding and Ultimate. *Aci Struct. J.* **2001**, *98*, 135–147. [[CrossRef](#)]
41. Moehle, J.P.; Lehman, D.E. Seismic Performance of Well-confined Confined Concrete Bridge Columns. *Spec. Publ.* **2000**, *238*. [[CrossRef](#)]
42. Tekeli, H.; Aydin, A. An experimental study on the seismic behavior of infilled RC frames with opening. *Sci. Iran.* **2017**. [[CrossRef](#)]
43. Wu, C.L.; Yang, Y.S.; Hwang, S.J.; Loh, C.H. Dynamic collapse of reinforced concrete columns. In *Proceedings of the 9th U.S. National and 10th Canadian Conference on Earthquake Engineering, Toronto, ON, Canada, 25–29 July 2010*.
44. Berry, M.; Eberhard, M. *Performance Models for Flexural Damage in Reinforced Concrete Columns*; University of California Berkeley: Berkeley, CA, USA, 2003.
45. Yun, H.W. Full-Scale Experimental and Analytical Studies on High-Strength Concrete Columns. Ph.D. Thesis, University of Southern California, Los Angeles, CA, USA, 2003.
46. Ho, J.C.M. Inelastic Design of Reinforced Concrete Beams and Limited Ductile High-Strength Concrete Columns. Ph.D. Thesis, The University of Hong Kong, Hong Kong, China, 2003.
47. Ongsupankul, S.; Kanchanalai, T.; Kawashima, K. Behavior of reinforced concrete bridge pier columns subjected to moderate seismic load. *ScienceAsia* **2007**, *33*, 175–185. [[CrossRef](#)]
48. Woodward, K.A.; Jirsa, J.O. Influence of Reinforcement on RC Short Column Lateral Resistance. *J. Struct. Eng.* **1984**, *110*, 90–104. [[CrossRef](#)]
49. Bayrak, O. Seismic Performance of Rectilinearly Confined High Strength Concrete Columns. Ph.D. Thesis, University of Toronto, Toronto, OT, Canada, 1999.
50. Mo, Y.L.; Wang, S.J. Seismic Behavior of RC Columns with Various Tie Configurations. *J. Struct. Eng.* **2000**, *126*, 1122–1130. [[CrossRef](#)]
51. Paultre, P.; Légeron, F.; Mongeau, D. Influence of concrete strength and transverse reinforcement yield strength on behavior of high-strength concrete columns. *ACI Struct. J.* **2001**, *98*, 490–501.
52. Xiao, Y.; Yun, H.W. Experimental studies on full-scale high-strength concrete columns. *ACI Struct. J.* **2002**, *99*, 199–207.

53. Lam, S.S.E.; Wang, Z.Y.; Liu, Z.Q.; Wong, Y.L.; Li, C.S.; Wu, B. Drift Capacity of Rectangular Reinforced Concrete Columns with Low Lateral Confinement and High-Axial Load. *J. Struct. Eng.* **2003**, *129*, 733–742. [[CrossRef](#)]
54. Hwang, S.K.; Yun, H.D. Effects of transverse reinforcement on flexural behaviour of high-strength concrete columns. *Eng. Struct.* **2004**, *26*, 1–12. [[CrossRef](#)]
55. Ahn, J.M.; Shin, S.W. An evaluation of ductility of high-strength reinforced concrete columns subjected to reversed cyclic loads under axial compression. *Mag. Concr. Res.* **2007**, *59*, 29–44. [[CrossRef](#)]
56. Woods, J.M.; Kioussis, P.D.; Ehsani, M.R.; Saadatmanesh, H.; Fritz, W. Bending ductility of rectangular high strength concrete columns. *Eng. Struct.* **2007**, *29*, 1783–1790. [[CrossRef](#)]
57. Marefat, M.S.; Khanmohammadi, M.; Bahrani, M.K.; Goli, A. Experimental Assessment of Reinforced Concrete Columns with Deficient Seismic Details under Cyclic Load. *Adv. Struct. Eng.* **2008**, *9*, 337–347. [[CrossRef](#)]
58. Xiao, X.; Guan, F.L.; Yan, S. Use of ultra-high-strength bars for seismic performance of rectangular high-strength concrete frame columns. *Mag. Concr. Res.* **2008**, *60*, 253–259. [[CrossRef](#)]
59. Bae, S. Seismic performance of full-scale reinforced concrete columns. *Aci Struct. J.* **2008**, *105*, 123–133.
60. Cao, T.N.T. Experimental and Analytical Studies on the Seismic Behavior of Reinforced Concrete Columns with Light Transverse Reinforcement. Ph.D. Thesis, Nanyang Technological University, Singapore, 2010.
61. Ou, Y.C.; Kurniawan, D.P.; Handika, N. Shear Behavior of Reinforced Concrete Columns with High-Strength Steel and Concrete under Low Axial Load. *ACI Mater. J.* **2015**, *112*, 35–45.
62. Abdelsamie, E.; Tom, B.; Salah, E. Plastic Hinge Length Considering Shear Reversal in Reinforced Concrete Elements. *J. Earthq. Eng.* **2012**, *16*, 188–210.
63. Martirosyan, A.; Xiao, Y. Flexural-Shear Behavior of High-Strength Concrete Short Columns. *Earthq. Spectra* **2012**, *17*, 679–695. [[CrossRef](#)]
64. Li, Y.A.; Huang, Y.T.; Hwang, S.J. Seismic Response of Reinforced Concrete Short Columns Failed in Shear. *Aci Struct. J.* **2014**, *111*, 945–954. [[CrossRef](#)]
65. Nakamura, T.; Yoshimura, M. Gravity load collapse of reinforced concrete columns with decreased axial load. In Proceedings of the 2nd European Conference on Earthquake Engineering and Seismology, Istanbul, Turkey, 25–29 August 2014.
66. Popa, V.; Cotofana, D.; Vacareanu, R. Effective stiffness and displacement capacity of short reinforced concrete columns with low concrete quality. *Bull. Earthq. Eng.* **2014**, *12*, 2705–2721. [[CrossRef](#)]
67. Jin, C.; Pan, Z.; Meng, S.; Qiao, Z. Seismic Behavior of Shear-Critical Reinforced High-Strength Concrete Columns. *J. Struct. Eng.* **2015**, *141*, 04014198. [[CrossRef](#)]
68. Bechtoula, H.; Kono, S.; Watanabe, F.; Mehani, Y.; Kibboua, A.; Naili, M. Performance of HSC columns under severe cyclic loading. *Bull. Earthq. Eng.* **2015**, *13*, 503–538. [[CrossRef](#)]
69. El-Attar, M.M.; El-Karmoty, H.Z.; El-Moneim, A.A. The behavior of ultra-high-strength reinforced concrete columns under axial and cyclic lateral loads. *HBRC J.* **2016**, *12*, 284–295. [[CrossRef](#)]

